NANO LETTERS

2005
Vol. 5, No. 9
1793−1796

Electric Field-Induced Magnetization Switching in Epitaxial Columnar Nanostructures

F. Zavaliche,*[,‡,§] H. Zheng,[†,‡] L. Mohaddes-Ardabili,[†,‡,||] S. Y. Yang,[‡,||] Q. Zhan,[‡] P. Shafer,[‡] E. Reilly,[⊥] R. Chopdekar,[‡] Y. Jia,[#] P. Wright,[⊥] D. G. Schlom,[#] Y. Suzuki,[‡] and R. Ramesh[‡]

Department of Materials Science and Engineering, and Department of Physics, University of California, Berkeley, Berkeley, California 94720, Materials Research Science and Engineering Center, University of Maryland, College Park, Maryland 20742, Department of Materials Science, University of Maryland, College Park, Maryland 20742, Department of Mechanical Engineering, University of California, Berkeley, Berkeley, California 94720, and Department of Materials Science and Engineering, Pennsylvania State University, University Park, Pennsylvania 16802

Received July 20, 2005; Revised Manuscript Received August 16, 2005

ABSTRACT

We present direct evidence for room-temperature magnetization reversal induced by an electric field in epitaxial ferroelectric $BiFeO_3$–ferrimagnetic $CoFe_2O_4$ columnar nanostructures. Piezoelectric force microscopy and magnetic force microscopy were used to locally image the coupled piezoelectric-magnetic switching. Quantitative analyses give a perpendicular magnetoelectric susceptibility of $\sim 1.0 \times 10^{-2}$ G cm/V. The observed effect is due to the strong elastic coupling between the two ferroic constituents as the result of the three-dimensional heteroepitaxy.

Materials which exhibit simultaneous magnetic and ferroelectric ordering, ferroelectro-magnets for short, have been the focus of scientists for decades due to their enticing technological potential.[1,2] The coupling between the corresponding order parameters was theoretically predicted long ago[3] and is currently a topic of intense interest. However, single phase materials which simultaneously show high magnetization and polarization at ambient conditions remain elusive.[4] Therefore, studies of such materials, e.g., manganites, have only been performed at low temperatures.[5−7] An alternative approach uses bonded magnetic and piezoelectric layers to investigate the room-temperature magnetoelectric coupling at macroscopic scales.[8,9]

In the present work, we utilize phase decomposition based self-assembly to create fully epitaxial nanocomposites of ferroelectric and magnetic oxides which enable controlled switching at the nanoscale. The intrinsic three-dimensional heteroepitaxy in such columnar nanostructures facilitates intimate lattice coupling.[10,11] To choose appropriate ferroelectric and magnetic materials for an epitaxial nanocomposite one needs to consider lattice match, chemical compatibility, solid solubility, and elastic properties. These factors were recently found to ultimately determine the morphology of the composite material[10], and implicitly its functionality.

The epitaxial nanostructure we investigated is a ∼200 nm thick film comprised of ferrimagnetic $CoFe_2O_4$ pillars embedded in a $BiFeO_3$ matrix, with a relative volume ratio of 35/65. We experimentally determined that increasing the amount of ferrimagnetic spinel phase at the expense of ferroelectric perovskite phase leads to some ordering of the magnetic phase.[10] We deliberately reduced the amount of $CoFe_2O_4$ in the present work, however, to enable local piezoelectric and magnetic characterization and manipulation by scanning probe microscopy techniques. The films were grown by pulsed laser deposition (PLD) on single crystalline (001) $SrTiO_3$ substrates (a = 3.91 Å) upon which a ∼50 nm thick $SrRuO_3$ bottom electrode (a = 3.93 Å) was grown, also by PLD. In bulk, spinel $CoFe_2O_4$ (a = 8.38 Å) exhibits a 4-fold magnetic anisotropy with the easy axis along ⟨001⟩, and a saturation magnetization of ∼350 emu/cm^3 (ref 12). $BiFeO_3$ possesses a rhombohedrally distorted perovskite

* To whom correspondence should be addressed. E-mail: zavaliche@berkeley.edu. Phone: (510)-643-8202. Fax: (510)-643-5792.
[†] These two authors contributed equally to this paper.
[‡] Department of Materials Science and Engineering, and Department of Physics, University of California, Berkeley.
[§] Materials Research Science and Engineering Center, University of Maryland.
[||] Department of Materials Science, University of Maryland.
[⊥] Department of Mechanical Engineering, University of California, Berkeley.
[#] Department of Materials Science and Engineering, Pennsylvania State University.

10.1021/nl051406i CCC: $30.25
Published on Web 08/26/2005

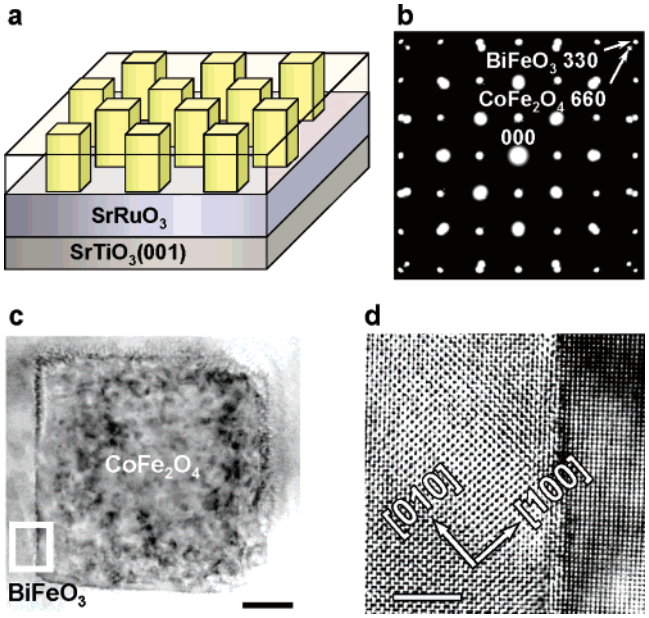

Figure 1. Structure and morphology of self-assembled $BiFeO_3-CoFe_2O_4$ epitaxial nanostructures. (a) A sketch of the heterostructure. (b) Typical selective area electron diffraction pattern. (c) Plan-view TEM image of a $CoFe_2O_4$ pillar surrounded by $BiFeO_3$. (d) High resolution plan-view TEM image of the $CoFe_2O_4-BiFeO_3$ interface taken in the area marked with a rectangle in c. The bars in c and d are 30 and 3 nm, respectively.

structure ($a_r = 3.96$ Å, $\alpha_r = 0.6°$)[13] and shows strong polarization and piezoelectric response[14].

Growth at elevated temperatures leads to phase separation and self-assembly of ferrimagnetic $CoFe_2O_4$ in columnar-like structures surrounded by ferroelectric $BiFeO_3$, as a consequence of very little mutual solid solubility of the two phases, depicted schematically in Figure 1a. This is manifested by the superposition of the corresponding electron diffraction spots in the selective area electron diffraction pattern shown in Figure 1b. Moreover, self-organization leads to nanostructuring of $CoFe_2O_4$ as rectangular pillars embedded into the $BiFeO_3$ matrix (Figure 1c). The epitaxial growth is inferred by the good lattice match between the components of the heterostructure and proven by the high-resolution electron micrograph shown in Figure 1d. The very good lattice and chemical match between $CoFe_2O_4$ and $BiFeO_3$ as well as between these two phases and the substrate leads to epitaxial alignment along the film's normal also.

Local magnetic and piezolectric response data acquired by magnetic force microscopy (MFM) and piezoelectric force microscopy (PFM)[15] (Figure 2a−c) prove that the ferroic properties of $CoFe_2O_4$ and $BiFeO_3$ are retained in the heterostructure. Thus, ferroelectricity and magnetism coexist in the thin film. We note that throughout this work, only nonmagnetic conducting probes were used for the contact-mode PFM scans, whereas magnetic probes were solely used for the tapping-lift MFM imaging (phase detection). The uniform magnetic contrast given by most of the pillars suggests that they are in a single-domain state, but polydomain magnetic structures are occasionally observed as well. In the images shown in Figure 2a,b the magnetic probe was magnetized in such a direction that white (positive phase, attractive interaction) stands for down magnetization, and black (negative phase, repulsive interaction) corresponds to up magnetization. Thus, magnetization points predominantly up in Figure 2a and down in Figure 2b. A perpendicular magnetic anisotropy was measured in the columnar $CoFe_2O_4$ structures, which can be attributed to the residual compressive strain, $\epsilon_{33}^{CoFe_2O_4} \sim 1.0 \times 10^{-3}$, as calculated from the electron diffraction data. A clear piezoelectric response is measured on the matrix by PFM (Figure 2c). Electrical poling was performed by scanning in contact mode with a conductive probe biased at −8 V over a $5 \times 5\ \mu m^2$ area, followed by another scan with the probe biased at +8 V over the central $3 \times 3\ \mu m^2$ area. The two tones observed in the perpendicular PFM image in Figure 2c indicate that the perpendicular component of polarization can be switched between two stable states in the $BiFeO_3$ matrix.

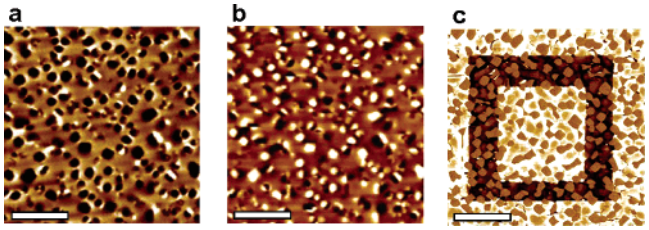

Figure 2. Magnetic and piezoelectric force microscopy images of a $(BiFeO_3)_{0.65}-(CoFe_2O_4)_{0.35}$ film. (a and b) Magnetic force microscopy images of the same area after magnetizing the film perpendicular to the surface in opposite magnetic fields of 20 kOe. (c) Perpendicular piezoelectric force microscopy image taken after poling the film at −8 V (dark frame), and +8 V (white, inside box). The bars are 2 μm.

MFM images of the same area shown in Figure 2a,b indicate that magnetization can be switched in the ferrimagnetic columns by applying a sufficiently strong magnetic field. The critical question is this: can an applied electric field switch/change the magnetization, i.e., is there a strong enough coupling between the two ferroic components of the nanocomposite? To explore this, PFM and MFM scans were taken after every electrical poling or magnetizing process. First, the film was magnetized out-of-plane in a 20 kOe magnetic field, which results in a predominantly upward-oriented magnetization in the $CoFe_2O_4$ columnar structures (white in Figure 3a). Second, the film was sequentially electrically poled at −12 and +12 V, and piezoelectric switching was confirmed by PFM. The difference between the MFM images taken before (Figure 3a) and after electrical poling (Figure 3b) is striking: a large fraction of the magnetic columnar structures fully reversed contrast from white to black, some partly changed color, and only a few remained unchanged. Such contrast reversal is illustrated in Figure 3c,d with line profiles taken over two such magnetic pillars before (black curves) and after electrical poling (red and green curves). The two colored curves correspond to the two magnetic entities marked with like colors in Figure 3a,b. From the line profiles in Figure 3c,d, we learn the following: (i) in the pillar marked with red, the MFM phase changed sign completely; (ii) in the pillar marked with green, the MFM phase only partly changed sign. Since sign changes in the MFM phase are the result of changes in the direction

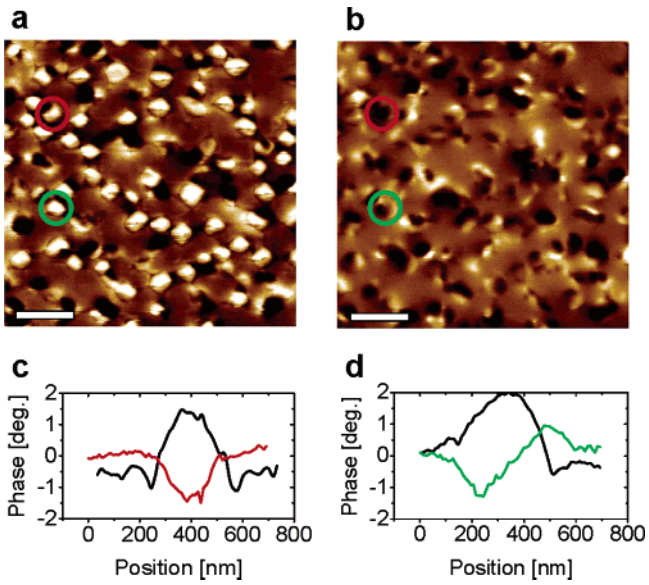

Figure 3. Changes in the magnetic configuration of a $(BiFeO_3)_{0.65}-(CoFe_2O_4)_{0.35}$ film upon electrical poling. Magnetic force microscopy image taken (a) after magnetization in an upward oriented 20 kOe perpendicular field, and (b) after electrical poling at +12 V. The bars are 1 μm. (c and d) Line profiles measured over two $CoFe_2O_4$ pillars emphasized in the MFM images with red and green, respectively. The black curves stand for the MFM signal before electrical poling.

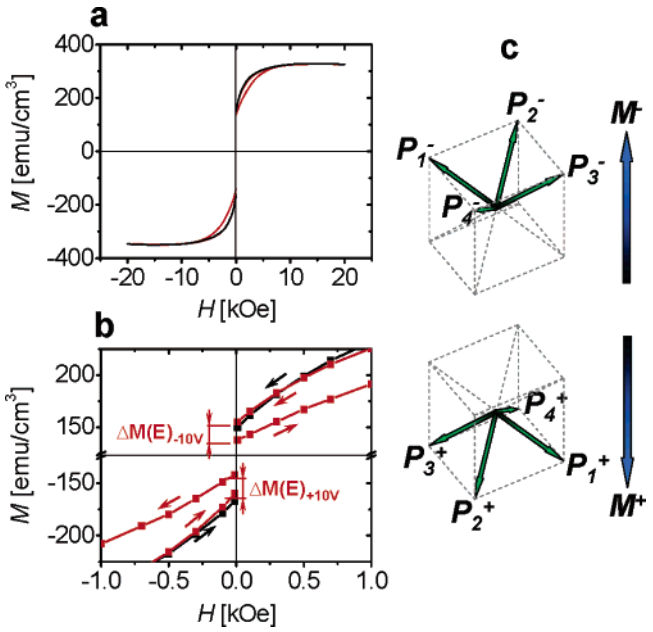

Figure 4. Quantitative analysis of magnetization change after electrical poling. (a) Magnetization curves taken before (black curves), and after (red curves) electrical poling of ~10% of the total film area. (b) An enlarged view of the central part of a. (c) Possible polarization/magnetization configurations for coupling.

of the magnetic interaction between probe and film (from attractive to repulsive in our case) the two situations depicted in Figure 3c,d correspond, respectively, to (i) magnetization reversal (red pillar in Figure 3a,b) and (ii) polydomain formation (green pillar in Figure 3a,b). We emphasize that this change in the state of magnetization in the magnetic columnar structures is solely the result of applying an electric field, implying a significant magnetoelectric coupling between the two ferroic components of the film. The electric-field induced switching of magnetization was also performed starting with the opposite magnetization direction in the pillars, i.e., pointing down, and similar results were obtained. Therefore, the two opposite perpendicular magnetization states in the $CoFe_2O_4$ columnar structures can be brought into each other by applying an electric field. This process can only be possible in the presence of a significant coupling between the ferroelectric matrix and ferrimagnetic pillars.

To quantify the strength of such a magnetoelectric coupling, 30 micron diameter test capacitors were fabricated over ~10% of the film area using a lithographic lift-off procedure. First, the film was magnetized in a downward oriented 20 kOe perpendicular magnetic field (positive in Figure 4). The resulting saturation to remanence $M(H)$ curve is depicted with a black line in Figure 4. All $M(H)$ curves in Figure 4 were measured by a superconducting quantum interference device (SQUID) magnetometer at room temperature. Afterward, the test capacitors were electrically poled with square, −10V pulses with a duration of 100 μs. Lower biases were applied on the deposited Pt contacts than that used in the PFM imaging experiments because better electrical contacts are achieved in the former case. Following electrical poling, the film was placed back in the SQUID magnetometer and the magnetization was measured again, ramping the field from 0 to 20 kOe and back to 0 (the red curve in Figure 4). Figure 4b shows an enlarged portion of the central part of the $M(H)$ plot in Figure 4a, in which the arrows point in the direction of field ramping. As the result of electrical poling at −10 V for 100 μs, the $M(H)$ curve starts from a value below remanence, M_r, and stays below the "saturation to remanence" curves up to about 7 kOe as the field is ramped up (red curve in the first quadrant of Figure 4b). Taking into account that only 10% of the film was poled, these SQUID measurements give a magnetization drop of $\sim 0.6 \times 2M_r$ in the columnar structures under the contacts, due to magnetization reversal or polydomain formation, as seen in the MFM image in Figure 3b. The same behavior is observed for the oppositely magnetized film (up) after poling at +10 V, (see the plots in the third quadrant in Figure 4, corresponding to negative fields).

The electric field-induced change of magnetization, ΔM, measured from the plots in Figure 4b enables us to estimate the strength of magnetoelectric coupling between the ferroelectric matrix and the ferrimagnetic columnar structures. We estimate the static perpendicular magnetoelectric susceptibility, $\alpha_{33} = \Delta M/\Delta E$, to be $\sim 1.0 \times 10^{-2}$ G cm/V. This value is indicative of significant coupling and agrees well with the numbers obtained for single crystalline piezoelectric−piezomagnetic bilayers at microwave frequencies.[9] In addition, it is important to note the potential to achieve spatial control of electric field-induced magnetization switching at the nanoscale. Two initial polarization/magnetization configurations were found to lead to the observed coupling effect upon the application of an electric field. These are schematically depicted in Figure 4c. $\mathbf{P}_i^{+/-}$, with $i = \overline{1,4}$ and $\mathbf{M}^{+/-}$ stand, respectively, for the eight possible orientations of

polarization in rhombohedral $BiFeO_3$[13] and two magnetization directions along (001) in spinel $CoFe_2O_4$.

The mechanism responsible for the electric field-induced magnetization switching involves the intimate lattice coupling between the two ferroic constituents of the nanocomposite, brought about by three-dimensional heteroepitaxial growth. In this picture, an electric field applied to the piezoelectric matrix leads to a change in its shape (through the converse piezoelectric effect) during switching, which dynamically alters the magnetic anisotropy of the ferrimagnetic pillars via their magnetostriction. At a certain applied bias, a perpendicular tensile strain is produced, which results in a harder perpendicular axis of magnetization in $CoFe_2O_4$ due to its negative magnetostriction, $\lambda_{333} = -350 \times 10^{-6}$ (ref 16). When this occurs, the magnetization can flip in-plane along any of the two easy axes and subsequently flips back to the perpendicular direction once the electrical bias is removed. Simple calculations show that the piezoelectric elastic energy density, $W_{el} \sim 0.6 \times 10^5$ J/m^3, is of the same order of magnitude as the magnetoelastic energy density, $W_{me} \sim 0.9 \times 10^5$ J/m^3, needed to be overcome to enable the temporary alteration of the magnetic anisotropy. The exact nature of the evolution of the magnetic structure in the nanopillars requires a detailed investigation of the coupling between converse piezoelectricity and magnetostriction in such nanostructures. These studies are currently in progress and will be reported in the future.

In summary, through the application of an electric field to a columnar ferroelectric/ferrimagnetic epitaxial nanocomposite, we have induced magnetization reversal. This result is possible because of a significant elastic strain-mediated magnetoelectric coupling between the two ferroic components of the nanocomposite, whose strength was estimated as $\sim 1.0 \times 10^{-2}$ G cm/V. The observation of such electric-field magnetization reversal at room-temperature opens new avenues for a number of applications ranging from energy conversion to information technology. To achieve full control over the electric-field induced switching of magnetization in each bit, the superposition of a weak perpendicular magnetic field during the electrical writing might be necessary. Finally, the implementation of heterostructures with similar architectures in useful devices requires the fulfillment of some technical requirements including low leakage and no crosstalk between the magnetic entities.

Acknowledgment. This work has been supported in part by the University of Maryland NSF-MRSEC under Grant No. DMR 00-80008, by the ONR under a MURI program, and by SRC under a MARCO program.

References

(1) Wood, Van E.; Austin, A. E. *Intl. J. Magn.* **1974**, *5*, 303.
(2) Scott, J. F. *Rev. Mod. Phys.* **1974**, *46*, 83.
(3) Landau, L. D.; Liftshitz, E. M. *Electrodynamics of continuous media*; Pergamon Press: Oxford, 1960; p 119.
(4) Hill, N. A. *J. Phys. Chem. B* **2000**, *104*, 6694.
(5) Fiebig, M.; Lottermoser, Th.; Fröhlich, D.; Goltsev, A. V.; Pisarev, R. V. *Nature* **2002**, *419*, 818.
(6) Lottermoser, Th.; Lonkai, Th.; Amann, U.; Hohlwein, D.; Ihringer, J.; Fiebig, M. *Nature* **2004**, *430*, 541.
(7) Kimura, T.; Goto, T.; Shintani, H.; Ishizaka, K.; Arima, T.; Tokura, Y. *Nature* **2003**, *426*, 55.
(8) Dong, S.; Li, J. F.; Viehland, D. *Philos. Mag. Lett.* **2003**, *83*, 769.
(9) Shastry, S.; Srinivasan, G.; Bichurin, M. I.; Petrov, V. M.; Tatarenko, A. S. *Phys. Rev. B* **2004**, *70*, 064416.
(10) Zheng, H.; Wang, J.; Lofland, S. E.; Ma, Z.; Mohaddes-Ardabili, L.; Zhao, T.; Salamanca-Riba, L.; Shinde, S. R.; Ogale, S. B.; Bai, F.; Viehland, D.; Jia, Y.; Schlom, D. G.; Wuttig, M.; Roytburd, A.; Ramesh, R. *Science* **2004**, *303*, 661.
(11) Nan, C.-W.; Liu, G.; Lin, Y.; Chen, H. *Phys. Rev. Lett.* **2005**, *94*, 197203.
(12) Smit, J.; Wijn, H. P. J. *Ferrites*; Wiley: New York, 1959; p 369.
(13) Kubel, F.; Schmid, H. *Acta Crystallogr.* **1990**, *B46*, 698.
(14) Wang, J.; Neaton, J. B.; Zheng, H.; Nagarajan, V.; Ogale, S. B.; Liu, B.; Viehland, D.; Vaithyanathan, V.; Schlom, D. G.; Waghmare, U. V.; Spaldin, N. A.; Rabe, K. M.; Wuttig, M.; Ramesh, R. *Science* **2003**, *299*, 1719.
(15) Gruverman, A.; Auciello, O.; Tokumoto, H. *Annu. Rev. Mater. Sci.* **1998**, *28*, 101.
(16) Folen, V. J. In *Magnetic and Other Properties of Oxides and Related Compounds*; Hellwege, K.-H., Hellwege, A. M., Eds.; Springer: Berlin, 1970; Landolt-Börnstein, vol. 3, part 4b, p 366.

NL051406I